Special Issue Article

Journal of
Intelligent Material
Systems and Structures

Multilayer piezoelectret foam stack for vibration energy harvesting

Journal of Intelligent Material Systems and Structures
2017, Vol. 28(3) 408–420

DOI: 10.1177/1045389X16657420
journals.sagepub.com/home/jim
SAGE

Chase A Ray and Steven R Anton

Abstract
Electronic devices are high-demand commodities in today's world, and such devices will continue increasing in popularity. Currently, batteries are implemented to provide power to these devices; however, the need for battery replacement, their cost, and the waste associated with battery disposal present a need for advances in self-powered technology. Energy harvesting technology has great potential to alleviate the drawbacks of batteries. In this work, a novel piezoelectret foam material is investigated for low-level vibration energy harvesting. Specifically, piezoelectret foam assembled in a multilayer stack configuration is explored. Modeling and experimentation of the stack when excited in compression at low frequencies are performed to investigate piezoelectret foam for multilayer energy harvesting. An equivalent circuit model derived from the literature is used to model the piezoelectret stack. Two 20-layer prototype devices and one 40-layer prototype device are fabricated and experimentally tested via harmonic base excitation. Electromechanical frequency response functions between input acceleration and output voltage are measured experimentally. Modeling results are compared to experimental measurements to assess the fidelity of the model near resonance. Finally, energy harvesting experimentation in which the device is subject to harmonic base excitation at the fundamental natural frequency is conducted to determine the ability of the stack to successfully charge a capacitor. For a 20-layer stack excited at 0.5 g, a 100-μF capacitor is charged to 1.45 V in 15 min, and produces a peak power of 0.45 μW. A 40-layer stack is found to charge a 100-μF capacitor to 1.7 V in 15 min when excited at 0.5 g, and produce a peak power of 0.89 μW.

Keywords
piezoelectret, multilayer stack, energy harvesting, electromechanical modeling

Introduction

Over the past few decades, one can readily observe that electronics are decreasing not only in size, but also in power consumption. The world is now full of small electronic devices, all of which require power in one way or another; be it from the power grid, from batteries, or from other sources. Many low-power sensors operate in the μW mW power range (Chao, 2011). Undoubtedly, the trend in reduction of power consumption is opening more opportunities for alternative energy sources for such low-power devices. Currently, batteries are the most widely used power source for two reasons: portability and power density. However, the main disadvantage of batteries is the need for periodic replacement. If sensors are placed in remote or inaccessible locations and the battery is depleted, then it can be costly, dangerous, or impossible to replace or recharge. This issue can be solved by replacing the battery with an energy harvester that scavenges energy from the local environment. The topic of energy harvesting has gained interest in the past decade with the adaptation of battery powered electronic devices. Evidence of the rise in popularity of energy harvesting can be found in the increasing number of publications, prototypes, and models in the literature (Anton and Sodano, 2007; Bogue, 2009; Cook-Chennault et al., 2008; Erturk and Inman, 2011; Priya and Inman, 2009; Ramadan et al., 2014).

One of the most highly researched energy harvesting mechanisms is piezoelectric transduction. Piezoelectric ceramic harvesters have been used in many cases and have been shown to provide sufficient power in many applications. An advantage of using piezoelectric ceramics is their high power output compared to other

Dynamic and Smart Systems Laboratory, Department of Mechanical Engineering, Tennessee Technological University, Cookeville, TN, USA

Corresponding author:
Steven R Anton, Dynamic and Smart Systems Laboratory, Department of Mechanical Engineering, Tennessee Technological University, Cookeville, TN 38505-0001, USA.
Email: santon@tntech.edu

types of vibration-based energy harvesting materials. On the other hand, a disadvantage is that ceramic piezoelectric materials are very rigid and dense. Under high loads and deflections, it is possible that the ceramic will fracture and render the device inoperable. Several piezoelectric polymers, including polyvinylidene fluoride (PVDF), active fiber composites (AFCs), and macro-fiber composites (MFCs), have been studied for energy harvesting and offer more compliant mechanical behavior compared to piezoelectric ceramics.

In this work, piezoelectret foam is investigated as an alternative to piezoceramic materials and other piezoelectric polymers, such as PVDF. The material is extremely compliant and light weight. Typical piezoelectret foam is only 70–100 μm thick and has a mass density around 1000 kg/m^3. Piezoelectricity is observed in piezoelectrets due to the deposition of charge on internal voids in the structure and the subsequent deformation of the charged voids under mechanical excitation. Additionally, piezoelectret foam has been shown to exhibit a piezoelectric constant up to seven times greater than PVDF (Hillenbrand et al., 2005). The compliance of piezoelectric polymers is the key feature that sets them apart from other vibration-based energy harvesters currently in research or practice. Piezoelectret foam can be attached to curved surfaces and manufactured or cut to any size to fit custom surfaces.

Over the past several decades, previous studies have described the development, fabrication, and evaluation of mechanical and electromechanical properties of piezoelectret foam (Bauer et al., 2004; Gerhard-Multhaupt, 2002; Kressmann, 2001; Ramadan et al., 2014; Savolainen and Kirjavainen, 1989; Wegener and Bauer, 2005). More recently, piezoelectret foam has been suggested for use in energy harvesting. Anton and Farinholt (2012a, 2012b) and Anton et al. (2014) first investigated the direct use of piezoelectret foam for energy harvesting by stretching samples in the length direction under harmonic excitation. Pondrom et al. (2014, 2015) presented the first studies on stacked piezoelectrets for energy harvesting in which multiple layers of piezoelectret film are stacked and excited directly in the thickness direction. Studies have also investigated the use of piezoelectret foam in harvesting energy from the human body during walking (Luo et al., 2015) and from arterial forces and throat motion (Wu et al., 2015). While polypropylene is the most common piezoelectret material studied (Wegener and Bauer, 2005), Wang et al. (2015) and Zhang et al. (2014, 2015) have investigated a new class of piezoelectret material, cross-tunnel fluoroethylenepropylene (FEP), for energy harvesting and showed improved thermal stability compared to polypropylene.

The goal of the research presented in this article is to investigate multilayer piezoelectret foam stacks for energy harvesting purposes. Recent studies by Pondrom et al. (2014, 2015) have investigated piezoelectret stacks ranging from 2 to 10 layers for energy generation and have shown improvements over a single-layer device. These studies focused on the power generation of the stacks through optimal load resistances in the order of tens to hundreds of MΩ. This work examines two 20-layer piezoelectret foam stacks (Stack 1 and Stack 2) and one 40-layer stack (Stack 3; composed of Stack 1 and Stack 2 connected mechanically in series and electrically in parallel) in order to achieve a more practical optimal load resistance. The piezoelectric d_{33} coefficient and voltage output of the stack across various load resistances are investigated as a function of excitation frequency through harmonic base excitation. Additionally, the power output is investigated as a function of load resistance for harmonic excitation at resonance. The modeling framework developed by Pondrom et al. (2014, 2015) is adapted to create an electromechanical model of the stacks. Results of simulations are compared to experimental measurements in order to validate the model around resonance. Finally, the energy harvesting performance of the stacks is investigated through capacitor charging experiments with harmonic excitation at the fundamental resonance of the fabricated devices.

Fabrication

Several different fabrication methods were investigated before the final procedure was selected. Presented in this study is a stack comprised of active layers of piezoelectret foam manufactured by Emfit Ltd (n.d.) and electrode/bonding layers of 3M double-sided adhesive copper tape. The final design is chosen due to the ease of fabrication and superior results when compared to alternative configurations explored that will not be presented here.

Preparation and assembly

The stack design places the foam layers mechanically in series and electrically in parallel. The parallel electrode configuration allows for a reduction of the optimal load resistance and an increase in the charge output. A representative schematic of the device configuration for a stack containing three layers can be seen in Figure 1 (the stacks fabricated in this study have 20 layers, so this schematic is repeated until the desired number of layers are obtained). The layer count of 20 chosen in this work represents a significant increase from previously published work, with the goal being to reduce the optimal load resistance to a more realistic value comparable to other vibration-based energy harvesters. Additionally, the layer count was restricted based on the maximum number of identical layers (in order to exclude variability) that could be produced from a

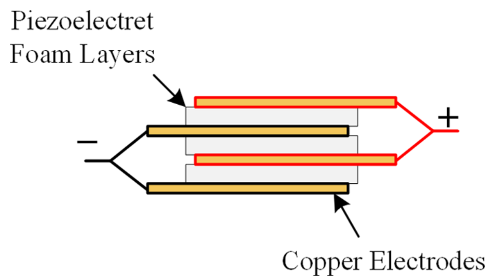

Figure 1. Schematic diagram of the piezoelectret foam stack showing layer configuration.

single sheet of piezoelectret foam acquired from the manufacturer.

The piezoelectret foam material used in this study is manufactured by Emfit Ltd (n.d.). Specifically, sheets of HS-06-20BR foam are used to prepare the stack. According to manufacturer specifications, the foam has a thickness of 80 μm, a piezoelectric constant of $d_{33} = 25 - 250\,\mathrm{pC/N}$, and a Young's modulus in the thickness direction of $Y_3 = 0.5\,\mathrm{MPa}$. Measurements were made on the foam and a mass density of 290 kg/m^3 was found. A single sheet of foam (as-supplied dimensions of 23 cm × 21 cm) is first cut into several 1.25 in. (3.175 cm) squares. The foam is cut slightly wider than the copper tape used for electrodes (which is 1 in (25.4 mm) wide) to prevent electrical shorting between layers. With the foam layers prepared, 3M model 1182 double-sided adhesive copper foil tape is applied between each layer to serve as both an electrode and an adhesive layer. According to manufacturer specifications, the copper backing has a thickness of 1.4 mil (0.04 mm), the total thickness of the tape (backing plus pressure sensitive acrylic adhesive on both sides) is 3.5 mil (0.088 mm), and the electrical resistance is 0.01 Ω. Furthermore, a mass density of 4091 kg/m^3 was measured for the foam. Placement of the copper electrodes requires great attention in order to achieve strong adhesion and no electrical shorting. Due to challenges in obtaining satisfactory conduction between all positive and all negative electrodes in preliminary designs, extended copper electrodes are used in the final design (Figure 2), with each layer receiving a successively shorter electrode. A final, single-sided adhesive copper layer (3M model 1181, measured mass density of 4859 kg/m^3) is placed on the exposed electrodes in order to ensure good conductivity between all layers and to prevent debris from adhering to the device. Finally, lead wires are soldered to the copper electrodes away from the foam layers to prevent adverse effects from high soldering temperatures. The fully assembled stack showing the extended electrodes can be seen in Figure 2. In this work, a total of two 20-layer stacks are fabricated (Stack 1 and Stack 2), and the two stacks are placed mechanically in series and electrically in parallel to form a 40-layer stack (Stack 3).

Mathematical modeling

The modeling framework described by Pondrom et al. (2014, 2015) is adapted in this work to model a multi-layer piezoelectret foam harvester as described in this section. A simple single degree-of-freedom model under harmonic base excitation is used to describe the mechanical behavior of the foam stack and to allow for parameter estimation. Electrically, the system is modeled using an equivalent circuit to determine the charge, voltage, and power produced by the stack.

Mechanical model

In this work, the piezoelectret foam stack is positioned between a vibrating base and a seismic mass in order to place the foam in direct compression (refer to the experimental setup given in Figure 5 and discussed later). The system is modeled as a single degree-of-freedom mass spring damper system under harmonic base excitation, as shown in Figure 3, where m_s is the total mass (which includes the seismic mass and the mass of the aluminum block used in the experiment

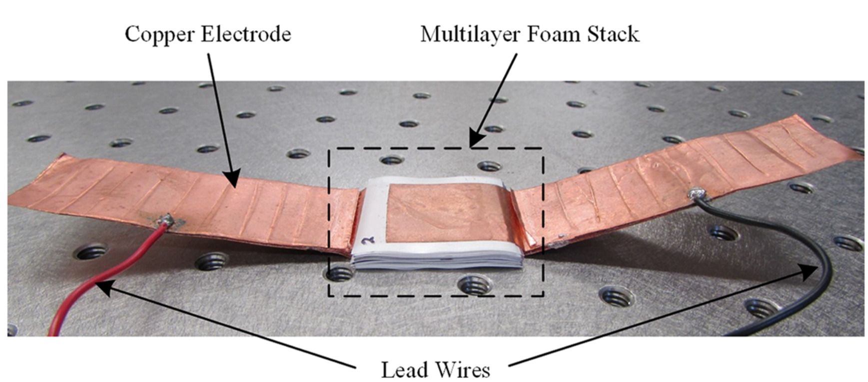

Figure 2. Depiction of the fully assembled piezoelectret foam stack.

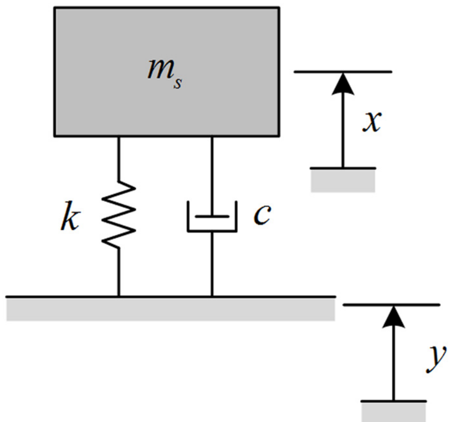

Figure 3. Mechanical model of the piezoelectret foam stack under base excitation.

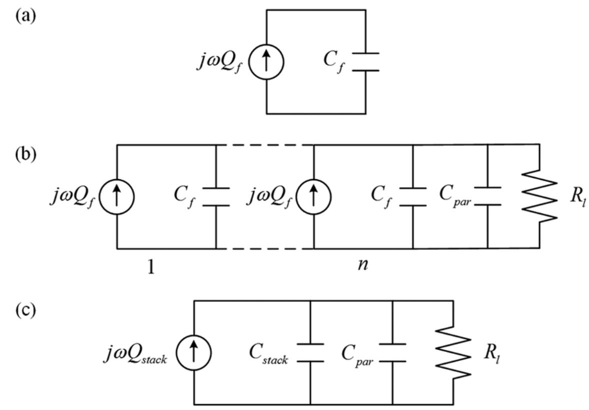

Figure 4. Circuit model adapted from Pondrom et al. (2014, 2015) for (a) single-layer piezoelectret foam, (b) piezoelectret foam stack connected electrically in parallel, and (c) equivalent circuit for multilayer piezoelectret foam stack connected electrically in parallel.

described later), and k and c represent the stiffness and damping of the stack, respectively.

The equation of motion of the base-excited piezoelectret foam stack can be written as follows

$$\ddot{x} + 2\zeta\omega_n\dot{x} + \omega_n^2 x = 2\zeta\omega_n\dot{y} + \omega_n^2 y \tag{1}$$

where x and y are the displacement of the seismic mass and base, respectively, ζ is the damping ratio of the stack, and ω_n is the natural frequency of the stack. Assuming harmonic base excitation of the form $y(t) = Ye^{j\omega t}$, the deflection of the stack, defined as $z(t) = x(t) - y(t)$, can be found by reformulating the base excitation problem in terms of $z(t)$, giving

$$z(t) = Ze^{j\omega t} = \frac{\omega^2 Ye^{j\omega t}}{\omega_n^2 - \omega^2 + j2\zeta\omega_n\omega} \tag{2}$$

where Z is the stack deflection, Y is the base (input) displacement, ω is the forcing frequency, j is the imaginary number, and t is the time. Additionally, the mass acceleration-to-base acceleration frequency response function (FRF) can be found from equation (1) (also under the assumption of harmonic base excitation) as

$$\frac{-\omega^2 Xe^{j\omega t}}{-\omega^2 Ye^{j\omega t}} = \frac{\omega_n^2 + j2\zeta\omega_n\omega}{\omega_n^2 - \omega^2 + j2\zeta\omega_n\omega} \tag{3}$$

where X is the seismic mass (output) displacement.

In order to develop an expression for the natural frequency of the stack, the following assumptions are made: (1) the mass of the stack layers is assumed to be negligible compared to the seismic mass; therefore, it is neglected (note, the stack mass is approximately 7.5 g compared to the seismic mass of 1.01 kg); (2) the stiffness of the copper electrode layers is much greater than the stiffness of the foam layers; therefore, the stiffness of the stack is dominated by the softer foam layers and can be approximated as several layers of foam connected mechanically in series; and (3) the effects of the adhesive layers on the stiffness of the stack are neglected. Using these assumptions, the natural frequency of the foam stack can be written as follows

$$\omega_n = \sqrt{\frac{E_f A}{nh_f m_s}} \tag{4}$$

where E_f is the modulus of elasticity of the foam, A is the cross-sectional area of the stack, n is the number of layers in the stack, and h_f is the thickness of a single layer of foam. It should be noted that the adhesive layers may have a non-negligible effect on the dynamic response of the stack; therefore, future work will also include the effects of the adhesive layers on the stiffness of the stack.

Electromechanical model

The piezoelectret stack is modeled electrically using the equivalent circuit shown in Figure 4(c). Each individual foam layer is modeled as a current generator that produces an alternating current (in response to harmonic mechanical excitation) of $j\omega Q_f$ in parallel with an internal capacitance, C_f, as shown in Figure 4(a). A multilayer stack with n layers connected electrically in parallel is represented in Figure 4(b), where all layers are assumed to be identical in terms of capacitance and generated current. A parasitic capacitance term, C_{par}, is included in parallel with the stack to model the parasitic capacitance associated with the test setup and measurement equipment. In Figure 4(c), an equivalent circuit is shown to represent a stack of piezoelectret foam as a current generator producing a current $j\omega Q_{stack}$ (where $Q_{stack} = nQ_f$) in parallel with a stack capacitance, C_{stack} (where $C_{stack} = nC_f$), the parasitic capacitance, C_{par}, and a load resistor, R_l.

The internal capacitance of a single layer is given by

$$C_f = \frac{\varepsilon A}{h_f} \tag{5}$$

where ε is the permittivity of the foam. For a single layer, the generator produces a current of $j\omega Q$ and the electric charge can be found by multiplying the piezoelectric coefficient by the stiffness of a single layer and the deflection of a single layer as follows

$$Q_f(t) = d_{33}\frac{E_f A}{h_f}\frac{z(t)}{n} \tag{6}$$

where d_{33} is the dynamic piezoelectric coefficient of a single layer. Equation (6) assumes that all deflection occurs in the foam layers and that the total deflection of the stack is evenly distributed among all foam layers. Combining equations (6), (4), and (2), the generated charge for a single layer in response to harmonic base excitation can be written as follows

$$Q_f(t) = \frac{d_{33} m_s \omega^2 Y e^{j\omega t}}{1 - (\omega/\omega_n)^2 + j2\zeta(\omega/\omega_n)} \tag{7}$$

In order to find the voltage produced by the stack, V_{stack}, Ohm's law can be applied. The impedance, Z_{eq}, of the equivalent circuit shown in Figure 4(c) is first found as

$$Z_{eq} = \frac{R_l}{1 + j\omega R_l (C_{stack} + C_{par})} \tag{8}$$

The generated stack current in short circuit is $I(t) = j\omega n Q_f(t)$. Combining this expression with equation (7) and equation (8) and applying Ohm's law one can arrive at the following voltage-to-base acceleration FRF of the stack

$$\frac{V_{stack} e^{j\omega t}}{-\omega^2 Y e^{j\omega t}} = \frac{-j\omega R_l d_{33}^{eff} m_s}{[1 - (\omega/\omega_n)^2 + j2\zeta(\omega/\omega_n)][1 + j\omega R_l (C_{stack} + C_{par})]} \tag{9}$$

where d_{33}^{eff} is the effective piezoelectric coefficient of a stack made of n identical layers connected electrically in parallel ($d_{33}^{eff} = nd_{33}$). Finally, using the power relation $P = V^2/R$, one can obtain the FRF for stack power, $P_{stack}(t)$, to the square of base acceleration as

$$\frac{P_{stack} e^{j2\omega t}}{\omega^4 Y^2 e^{j2\omega t}} = \frac{\omega^2 R_l {d_{33}^{eff}}^2 m_s^2}{\{[1 - (\omega/\omega_n)^2 + j2\zeta(\omega/\omega_n)][1 + j\omega R_l (C_{stack} + C_{par})]\}^2} \tag{10}$$

Experimental characterization

Electromechanical testing is performed on the fabricated piezoelectret foam stacks in order to characterize their behavior. The effective dynamic piezoelectric constant, d_{33}^{eff}, of the stacks is first measured as a function of frequency. A frequency range of 10 Hz–1 kHz is chosen to encompass the majority of ambient excitation frequencies found in macro-scale energy harvesting systems. Mechanical (mass acceleration-to-base acceleration) and electrical (voltage-to-base acceleration) FRFs are next measured and compared to simulation results to validate the model. Finally, the energy harvesting performance of the piezoelectret stacks is investigated by subjecting the devices to harmonic base excitation at their natural frequency and allowing the stacks to charge a capacitor using a simple rectifying circuit. The various experimental test setups and results are described in the following sections.

Effective dynamic piezoelectric constant testing

An experimental setup similar to that used previously by the authors (Anton et al., 2014) is implemented in this study for the measurement of the effective dynamic piezoelectric constant, d_{33}^{eff}. Figure 5 shows the schematic of the setup which depicts a foam stack being excited by an electromagnetic shaker in the vertical orientation. The charge output is monitored during excitation using a custom written LabVIEW program run in conjunction with a National Instruments CompactDAQ data acquisition device and a PCB 464A charge amplifier. An Agilent 33220A function generator is used to generate the excitation signal to the shaker which is run through a Labworks pa-138 power amplifier to a Labworks ET-139 shaker.

The foam stack is positioned centrally on top of a flat fixture that is connected directly to the armature of the shaker. On top of the foam sits a 1×1 in^2 (25.4×25.4 mm^2) block of aluminum. A 1 kg seismic mass along with a PCB 352C22 teardrop accelerometer is placed on top of the aluminum block. Care is taken to ensure that the stack, aluminum block, and seismic mass are all aligned directly above the shaker armature. In addition, a layer of Kapton tape is used to electrically insulate the stack from the aluminum fixture and seismic mass. The signal from the foam stack is sent through the charge amplifier to a NI-9215 data acquisition card, and the accelerometer signal is sent directly to a NI-9234 data acquisition card, both of which are monitored in real time.

The excitation frequency is varied logarithmically by the function generator from 10 Hz to 1 kHz. Two main forces act on the foam stack while being excited: dynamic force and static force. Gravity causes the static force, f_s, and the acceleration from the vibrating seismic

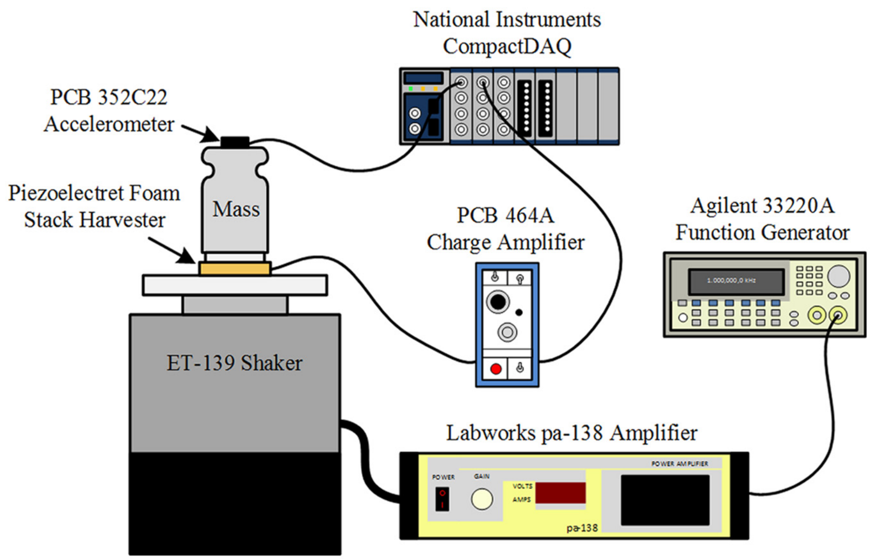

Figure 5. Experimental setup used to determine dynamic piezoelectric constant.

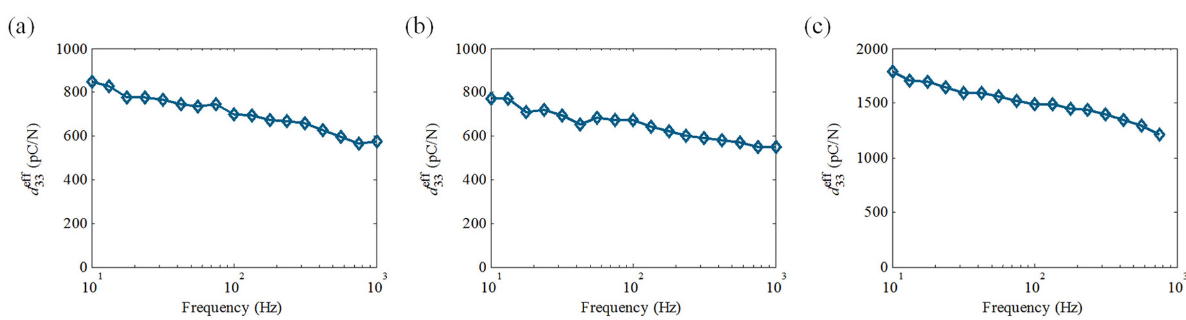

Figure 6. Results of effective dynamic piezoelectric coefficient testing for (a) Stack 1 (20 layers), (b) Stack 2 (20 layers), and (c) Stack 3 (40 layers).

mass causes the dynamic force, f_d. With this setup, a note should be made that the g-level cannot exceed 1 g. If 1 g is exceeded, then contact between the seismic mass and the aluminum fixture will be periodically lost; therefore, the excitation level is limited to 0.5 g in this work. The effective dynamic piezoelectric constant, d_{33}^{eff} (C/N), is found directly by dividing the charge output of the piezoelectric stack by the dynamic force measured with the accelerometer. Results from dynamic d_{33}^{eff} testing are given in Figure 6. The measurements show that d_{33}^{eff} exhibits slight frequency dependence, with the value decreasing with increasing frequency. These results are consistent with the frequency-depended behavior reported previously in the literature (Hillenbrand and Sessler, 2000; Kressmann, 2001).

To provide a general measure of d_{33}^{eff} for the foam stacks and to allow comparison to published manufacturer specifications, the average d_{33}^{eff} values across all frequencies tested for Stack 1, Stack 2, and Stack 3 are calculated as 704, 649, and 1513 pC/N, respectively. These lead to equivalent single-layer d_{33} values for Stack 1, Stack 2, and Stack 3 of 35.2, 32.5, and 37.8 pC/N, respectively. According to the manufacturer's specifications, d_{33} values for a single layer may range from 25 to 250 pC/N (Emfit Ltd (n.d.)); therefore, measured data are in agreement with the manufacturer's specifications. Note, Stack 1 and Stack 2 are intended to be identical; however, differences are found and can be attributed to the fact that each stack is made from a different sheet of foam and there are inconsistencies in the foam manufacturing process, as well as inconsistencies in the stack fabrication process.

Mechanical testing

The mechanical FRFs of the stacks are measured in order to empirically determine their damping coefficients and natural frequencies for use in the mechanical model given in equation (3). Once obtained, modeling results are then compared to experimental results to validate the model. The experimental setup used for acquiring the mechanical FRFs is shown in Figure 7.

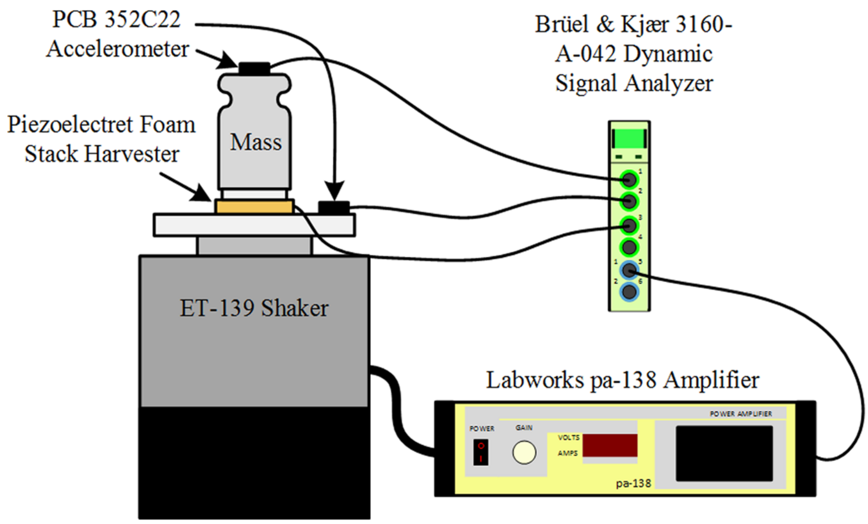

Figure 7. Experimental setup used for mechanical and electromechanical frequency response function measurements.

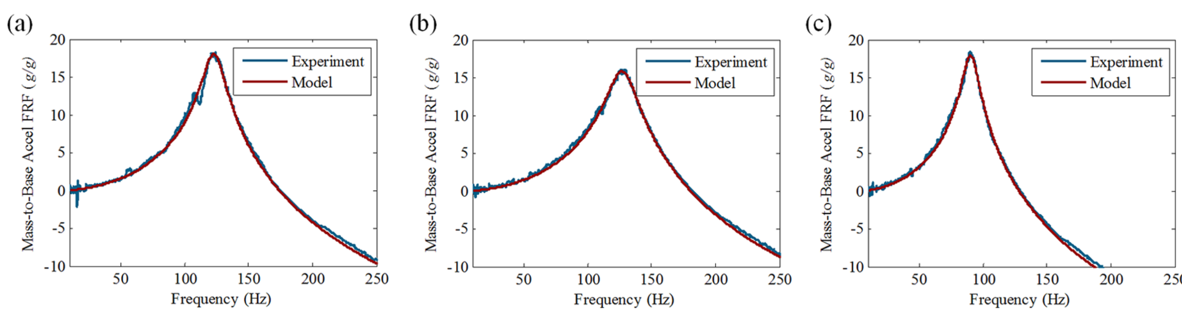

Figure 8. Mechanical frequency response functions for (a) Stack 1 (20 layers), (b) Stack 2 (20 layers), and (c) Stack 3 (40 layers).

The measurements are taken using a Brüel & Kjær 3160-A-042 dynamic signal analyzer by sweeping the excitation frequency and monitoring the response of the accelerometer placed on the mass and the response of the accelerometer placed on the base in order to calculate mass-to-base acceleration FRFs. Results of the testing for all three stacks are presented in Figure 8. Recall, the foam stacks are modeled as single degree-of-freedom systems; therefore, it is expected that discrepancies will be observed for frequencies above the fundamental resonance frequency where the model is unable to predict the contribution from higher order modes. In this analysis, focus is placed on analyzing the system around the fundamental frequency where maximum energy can be harvested. From the response plots shown, the damping ratio is found using the half-power bandwidth method for viscous damping using the formula (Ewins, 2000)

$$\zeta = \frac{\omega_2 - \omega_1}{2\omega_n} \tag{11}$$

where ζ is the damping ratio, ω_1 and ω_2 are the frequencies at which the amplitude is 3 dB less than the resonance peak to the left and right of the peak, respectively, and ω_n is the natural frequency. Note, due to the lack of smoothness of the response and the approximation of a single degree-of-freedom system, some errors occur when using this method of extracting information from the frequency response plots. In order to help reduce this error, the data are smoothed and a least squares fit is performed between the smoothed data and model around the resonance frequency with a bandwidth of 10 Hz, expressed by

$$err = \sum_{i=1}^{N} (x_{exp,i} - x_{sim,i})^2 \tag{12}$$

where N is the number of points in the fit, $x_{exp,i}$ is the experimental value at a frequency i, and $x_{sim,i}$ is the simulation value at the corresponding frequency. This iterative process begins with the damping ratio found from the experimental data using equation (11) and gradually adjusts the damping ratio used in the model until the lowest error is achieved between experiment and model. Results for the calculated damping ratios are shown in Table 1 along with the resonance frequencies extracted from the experimental results. Additionally,

Table 1. Natural frequency and damping coefficient values found empirically from FRF plots, and measured stack capacitance values.

	ω_n (Hz)	ζ	C_{stack} (pF)
Stack 1	123.3	0.063	1558
Stack 2	127.8	0.082	1498
Stack 3	90.6	0.064	3000

each stack's capacitance is measured directly using a BK Precision model 879 LCR meter and the results are also shown in the table. The mechanical model given by equation (3) is used to simulate the frequency response of the stack and results are also plotted in Figure 8 for comparison to the experimental data. From the figure, good agreement between measured and modeled data can be seen, particularly around resonance. It should be noted that the response for Stack 1 and Stack 2 differs appreciably although the stacks are intended to be identical. From Table 1, it can be seen that the damping ratio of Stack 2 is approximately 30% larger than Stack 1, which explains why Stack 2 underperforms Stack 1 at resonance. Again, the differences between Stack 1 and Stack 2 are attributed to inconsistencies in the foam manufacturing process as well as the stack fabrication process.

Electromechanical testing

Electromechanical testing is performed to determine the relationship between the input excitation and the voltage output of the piezoelectret foam stacks. Voltage-to-base acceleration FRFs are measured over a range of load resistances in order to characterize the performance of the stacks and to determine the optimal load resistances such that maximum power output can be obtained. The experimental setup used for electromechanical testing is also shown in Figure 7 and is nearly identical to that used for mechanical FRF testing with the exception that the voltage output across a load resistance (resistor not shown) along with the base acceleration is monitored. Again, frequency sweeps are performed from 10 Hz to 1 kHz. Nine load resistances are tested in the range of 400 kΩ to 5 MΩ.

Results of the voltage-to-base acceleration FRF measurements are given in Figure 9 along with simulation results using equation (10). It should be noted that the frequency-depended values of d_{33}^{eff} presented in Figure 6 are used in the model. For clarity, only three of the resistors used in the sweep are shown in the figure. Overall, there is good agreement between the model and the experimental data around resonance with errors typically in the order of 4% (maximum error of 10.8%) considering all nine load resistances tested. The model developed in the study is a single degree-of-freedom model, which is a simplification of the physical stack harvester; therefore, the effects of higher order modes cannot be captured. This explains the discrepancies seen in Figure 9 at high frequencies

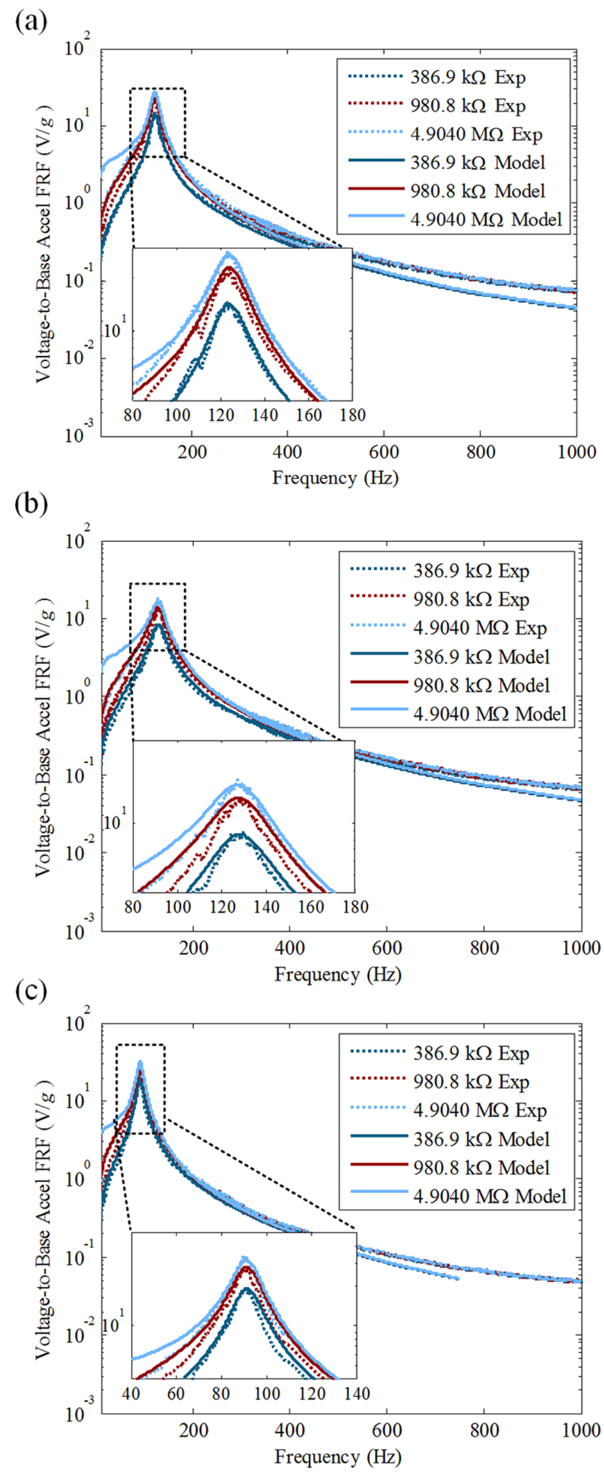

Figure 9. Voltage-to-base acceleration frequency response functions showing experimental (dashed lines) and model (solid lines) results for three load resistances for (a) Stack 1 (20 layers), (b) Stack 2 (20 layers), and (c) Stack 3 (40 layers).

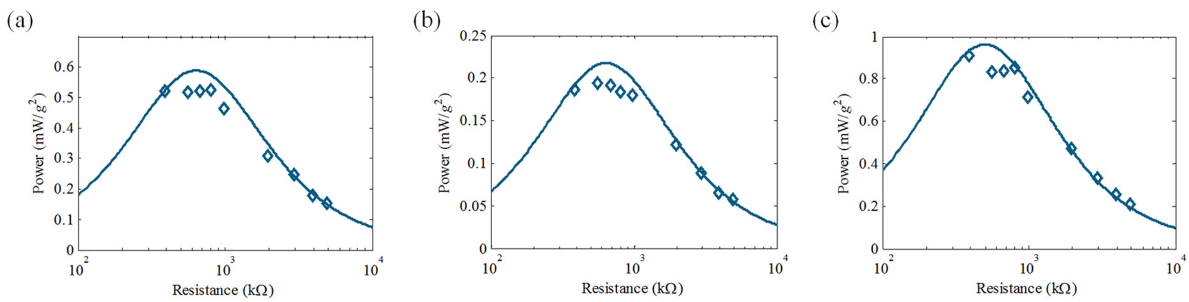

Figure 10. Experimental (markers) and analytically (line) peak power output versus load resistance diagram for excitation at the natural frequency (normalized with respect to base acceleration squared) for (a) Stack 1 (20 layers) excited at 123.3 Hz, (b) Stack 2 (20 layers) excited at 127.8 Hz, and (c) Stack 3 (20 layers) excited at 90.6 Hz.

above the first mode. For energy harvesting purposes, however, the stacks are excited at the natural frequency to obtain maximum power output; thus, the primary goal is to develop a model that represents the stack behavior near resonance. The inaccuracies at low frequencies are not of significant concern. Overall, the results prove the ability of the model to predict the electrical output of the stacks around resonance, thereby validating the model in this region.

The electrical power output (normalized with respect to base acceleration squared) for excitation at the natural frequency (see Table 1 for natural frequencies) for all nine load resistances tested is extracted from the voltage-to-base acceleration FRFs to compare model predictions and experimental measurements of the peak AC power output of the piezoelectret foam stacks. The resulting power output versus load resistance for each stack is shown in Figure 10 for both experimental results and simulation using equation (10). From the results, the model matches the experimental data well; however, some discrepancies are found near the optimal load resistance, with the model over predicting the power output. Despite these discrepancies, the model does well in predicting the overall behavior of the stack power output as a function of load resistance. Peak power outputs are measured for Stack 1, Stack 2, and Stack 3 as 0.52 mW/g^2 at 802.5 kΩ, 0.19 mW/g^2 at 556.7 kΩ, and 0.91 mW/g^2 at 386.9 kΩ, respectively, and modeled as 0.59 mW/g^2 at 639.8 kΩ, 0.22 mW/g^2 at 634.9 kΩ, and 0.96 mW/g^2 at 506.1 kΩ, respectively. Of interest is to note the difference in performance of Stack 1 and Stack 2. Stack 2 generates about 60% less peak power compared to Stack 1. This is consistent with the lower d_{33}^{eff} values observed (Figure 6) and the lower mechanical and electrical response at resonance (see Figures 8 and 9, respectively). Again, this is attributed to differences in the foam manufacturing and stack fabrication processes.

Energy harvesting

In order to evaluate the energy harvesting capabilities of piezoelectret foam in a stack configuration, tests are conducted in which the stacks are used to charge a capacitor. A setup similar to that used for dynamic d_{33}^{eff} testing (shown in Figure 5) is used here for the energy harvesting experiments. The stacks are excited harmonically at resonance at 0.5 g and the voltage output is conditioned using a full-wave diode rectifier bridge circuit to provide DC output. The diode bridge contains Schottky diodes to minimize the forward voltage drop across the bridge. A range of capacitors are then charged using the quasi-DC output of the bridge, and the voltage history is recorded in LabVIEW using an NI-9215 data acquisition card. In this article, results from charging a 100 µF and a 1000 µF capacitor using all three fabricated stacks are provided. The experimental capacitor charging time histories for measured voltage, calculated current, and calculated power are shown in Figures 11 to 13 for Stack 1, Stack 2, and Stack 3, respectively.

Stack 1 (20 layers) is able to charge a 100 µF capacitor to approximately 1.45 V in approximately 15 min. Consequently, this produces a maximum power of approximately 0.45 µW. For a 1000 µF capacitor, Stack 1 is able to charge it to approximately 1.2 V in 1 h. The calculated maximum power for this scenario is approximately 0.4 µW.

Stack 2 (20 layers) has the ability to charge a 100 µF capacitor to 0.92 V in about 15 min. In turn, a maximum power of 0.20 µW is produced. For a 1000 µF capacitor, Stack 2 is able to charge it to approximately 0.86 V in 1 h. The calculated maximum power for this scenario is also just over 0.20 µW. As discussed before, Stack 1 was shown to outperform Stack 2 and this conclusion is confirmed by the capacitor charging results presented here. Furthermore, the results show the extent of the variation between Stack 1 and Stack 2, with Stack 2 producing only half of the maximum power of Stack 1, which can be used to conclude that variations in either fabrication or the properties of individual sheets of piezoelectret foam can cause significant variations in performance of a stack harvester.

Finally, Stack 3 (40-layer, parallel electrode connection), which is expected to outperform the other two

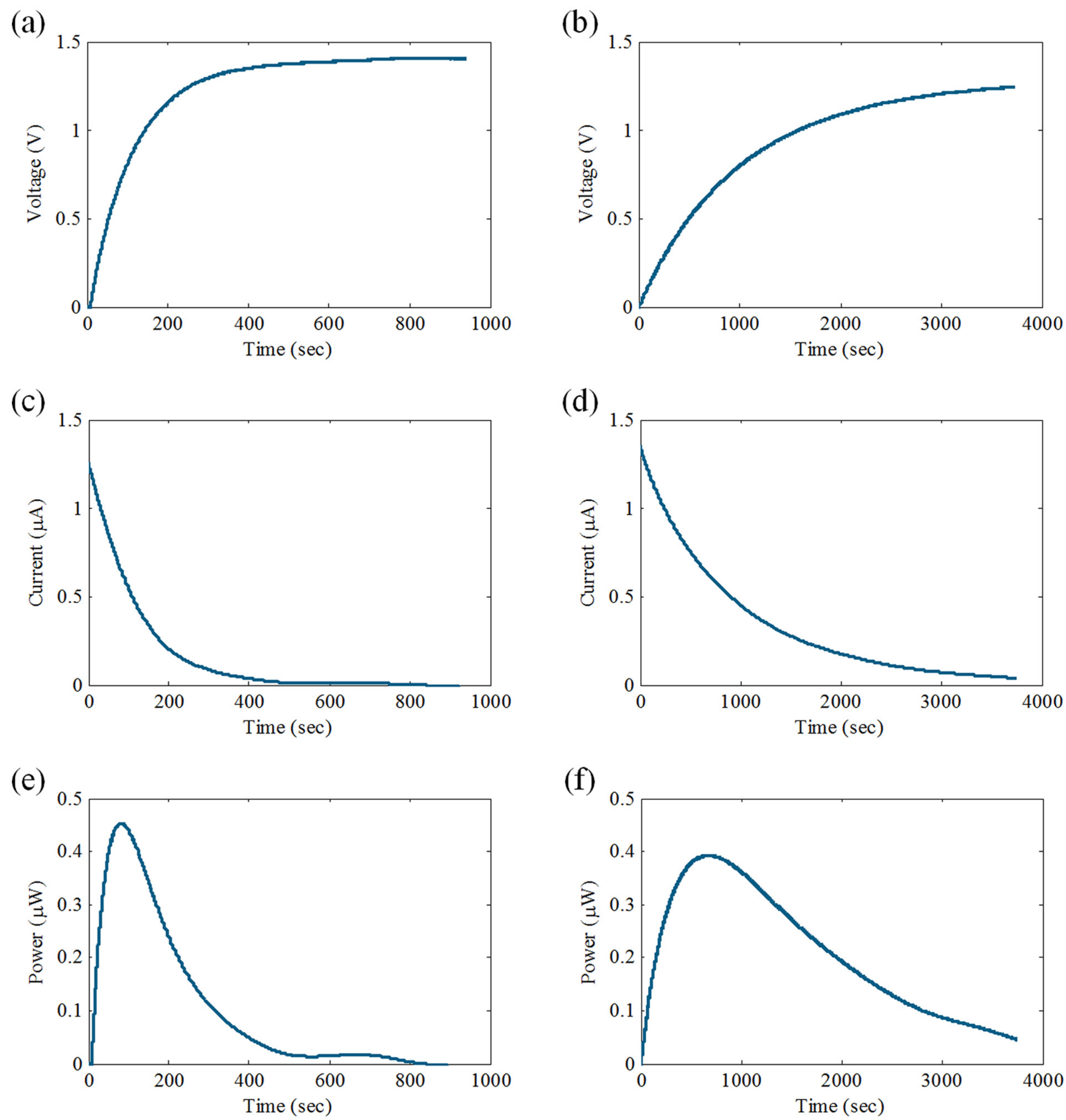

Figure 11. Energy harvesting results for Stack 1 (20 layers) showing (a) voltage history, (c) calculated current, and (e) calculated power for a 100 μF capacitor; and (b) voltage history, (d) calculated current, and (f) calculated power for a 1000 μF capacitor.

stacks, is able to charge a 100 μF capacitor to approximately 1.7 V in roughly 15 min. This produces a maximum power of around 0.89 μW. In the case of the 1000 μF capacitor, Stack 3 is able to charge it to 1.68 V also, but in about 90 min. This in turn produces a maximum power of approximately 0.84 μW.

Based on the results presented in the figures, it is clear that a well-performing 20-layer piezoelectret foam stack is capable of charging the capacitors to above 1.2 V and producing in the order of 0.4 μW. Furthermore, the 40-layer stack can charge the capacitors to 1.7 V and produce around 0.8 μW. Overall, the results presented are promising and suggest that a piezoelectret foam stack is capable of generating enough energy to charge a small capacitor that can be used to power a low-power electronic device. Additionally, when fabricated with more layers or a larger cross-sectional area, the output power of the stacks can be increased.

Discussion and conclusion

In this work, the use of piezoelectret foam in a stack configuration as a novel approach for low-level

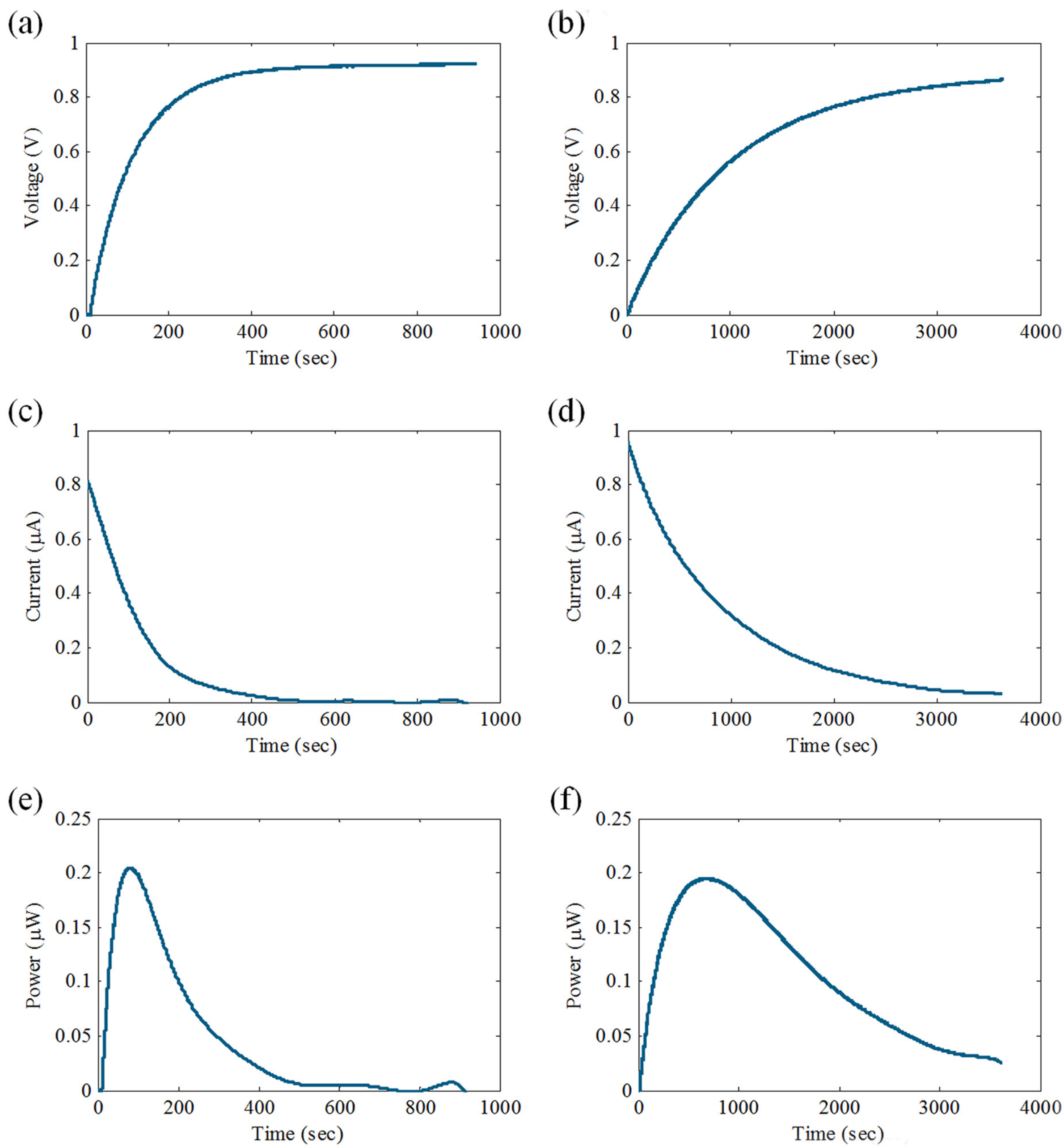

Figure 12. Energy harvesting results for Stack 2 (20 layers) showing (a) voltage history, (c) calculated current, and (e) calculated power for a 100 μF capacitor; and (b) voltage history, (d) calculated current, and (f) calculated power for a 1000 μF capacitor.

vibration energy harvesting applications is investigated. Piezoelectret foams operate based on changes in their thickness, which compress or stretch the macroscopic dipoles created during the fabrication process, thereby creating charge flow and providing piezoelectric-like response. Several aspects of the foam stacks have been investigated. Fabrication of 20-layer piezoelectret foam stacks is first described. Electromechanical modeling is then performed to predict the behavior of the foam stacks under harmonic base excitation. A modeling framework presented recently in the literature is adapted for use in this work and consists of modeling the stack mechanically as a single degree-of-freedom base-excited system and electrically as a current source in parallel with a capacitance. Electromechanical testing is then performed in order to measure the dynamic d_{33}^{eff} coefficient of each fabricated stack under a 1 kg seismic mass. The average d_{33}^{eff} values are found to be 704, 649, and 1513 pC/N for Stack 1 (20 layers), Stack 2 (20 layers), and Stack 3 (40-layer, combination of Stack 1 and Stack 2), respectively. In addition, the dynamic d_{33}^{eff} coefficient is found to be slightly frequency dependent for each stack, which is consistent with the literature. The average value for the dynamic

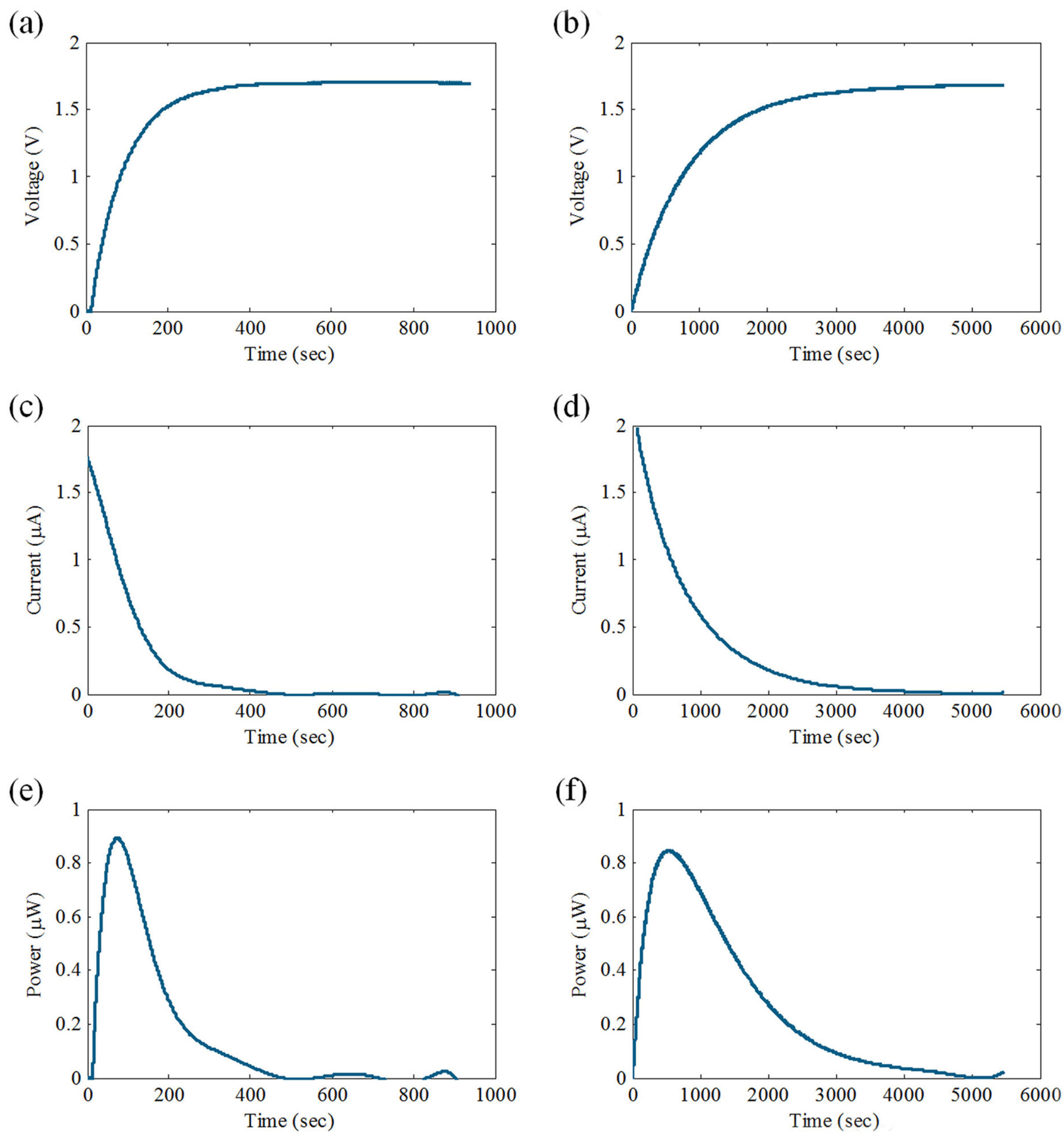

Figure 13. Energy harvesting results for Stack 3 (40 layers) showing (a) voltage history, (c) calculated current, and (e) calculated power for a 100 μF capacitor; and (b) voltage history, (d) calculated current, and (f) calculated power for a 1000 μF capacitor.

d_{33} coefficient per layer agrees with the manufacturers specifications for a single layer. Next, mechanical mass-to-base acceleration FRFs are found to empirically obtain the damping coefficient and natural frequency of the foam stacks, and simulation predictions using the model presented in this work are compared with the measured data. Comparisons show good matching around resonance, thereby validating the model in this region. It should be noted that due to the single degree-of-freedom nature of the model, simulations are unable to capture the effects of higher order modes; however, the region around resonance is of most importance for energy harvesting consideration. Electromechanical voltage-to-base acceleration FRFs are then found for a range of load resistances between 400 kΩ and 5 MΩ, and each measurement is compared to simulation results for validation of the model. All FRFs show good agreement between experiment and model near resonance with errors around 4%. Finally, the energy harvesting ability of piezoelectret foam is investigated experimentally. Under harmonic base excitation at resonance with an acceleration of 0.5 g using a 1 kg seismic mass, a 20-layer stack (Stack 1) is found to produce a peak power output of 0.45 μW and charge a

100 μF capacitor to 1.45 V in 15 min, and a 40-layer stack (Stack 3) is found to produce a peak power of 0.89 μW and charge a 100 μF capacitor to 1.7 V in 15 min. This voltage level is sufficient for powering low-power electronic devices. In conclusion, piezoelectret foam stacks show promise for use in low-level vibration energy harvesting applications as lead-free and extremely compliant alternatives to conventional piezoceramic materials. For future work, possible areas of improvement include increasing the stack cross-sectional area, increasing the number of layers in the stack, combining multiple stacks electrically in series, exploring alternative adhesion media between layers to promote compliance of the assembly, improving the mechanical and electrical circuit models, and designing an optimal circuit for maximum efficiency of energy transfer between the harvester and the storage medium.

Declaration of conflicting interests

The author(s) declared no potential conflicts of interest with respect to the research, authorship, and/or publication of this article.

Funding

The author(s) received no financial support for the research, authorship, and/or publication of this article.

References

Anton SR and Farinholt KM (2012a) An evaluation on low-level vibration energy harvesting using piezoelectret foam. In: *Proceedings of the 19th SPIE annual international symposium on smart structures and materials and nondestructive evaluation and health monitoring*, San Diego, CA, 11 March, 83410G (10 pp.). Bellingham, WA: SPIE.

Anton SR and Farinholt KM (2012b) Piezoelectret foam-based vibration energy harvester for low-power energy generation. In: *Proceedings of the ASME 2012 conference on smart materials, adaptive structures and intelligent systems*, Stone Mountain, GA, 19–21 September, SMASIS2012-S8224 (9 pp.). New York: ASME.

Anton SR and Sodano HA (2007) A review of power harvesting using piezoelectric materials (2003–2006). *Smart Materials and Structures* 16(3): R1–R21.

Anton SR, Farinholt KM and Erturk A (2014) Piezoelectret foam-based vibration energy harvesting. *Journal of Intelligent Material Systems and Structures* 25(14): 1681–1692.

Bauer S, Gerhard-Multhaupt R and Sessler G (2004) Ferroelectrets: soft electroactive foams for transducers. *Physics Today* 57(2): 37–43.

Bogue R (2009) Energy harvesting and wireless sensors: a review of recent developments. *Sensor Review* 29(3): 194–199.

Chao PC (2011) Energy harvesting electronics for vibratory devices in self-powered sensors. *IEEE Sensors Journal* 11(12): 3106–3121.

Cook-Chennault KA, Thambi N and Sastry AM (2008) Powering MEMS portable devices—a review of non-regenerative and regenerative power supply systems with special emphasis on piezoelectric energy harvesting systems. *Smart Materials and Structures* 17(4): 043001 (33 pp.).

Emfit Ltd (n.d.) Available at: https://www.emfit.com/ (accessed 8 September 2015).

Erturk A and Inman DJ (2011) *Piezoelectric Energy Harvesting*. Chichester: John Wiley & Sons, Ltd.

Ewins DJ (2000) *Modal Testing: Theory, Practice, and Application*. Baldock: Research Studies Press Ltd.

Gerhard-Multhaupt R (2002) Less can be more. Holes in polymers lead to a new paradigm of piezoelectric materials for electret transducers. *IEEE Transactions on Dielectrics and Electrical Insulation* 9(5): 850–859.

Hillenbrand J and Sessler GM (2000) Piezoelectricity in cellular electret films. *IEEE Transactions on Dielectrics and Electrical Insulation* 7(4): 537–542.

Hillenbrand J, Sessler GM and Zhang X (2005) Verification of a model for the piezoelectric d33 coefficient of cellular electret films. *Journal of Applied Physics* 98(6): 064105 (5 pp.).

Kressmann R (2001) Linear and nonlinear piezoelectric response of charged cellular polypropylene. *Journal of Applied Physics* 90(7): 3489–3496.

Luo Z, Zhu D, Shi J, et al. (2015) Energy harvesting study on single and multilayer ferroelectret foams under compressive force. *IEEE Transactions on Dielectrics and Electrical Insulation* 22(3): 1360–1368.

Pondrom P, Hillenbrand J, Sessler GM, et al. (2014) Vibration-based energy harvesting with stacked piezoelectrets. *Applied Physics Letters* 104(17): 172901 (5 pp.).

Pondrom P, Hillenbrand J, Sessler GM, et al. (2015) Energy harvesting with single-layer and stacked piezoelectret films. *IEEE Transactions on Dielectrics and Electrical Insulation* 22(3): 1470–1476.

Priya S and Inman DJ (2009) *Energy Harvesting Technologies*. New York: Springer Science + Business Media LLC.

Ramadan KS, Sameoto D and Evoy S (2014) A review of piezoelectric polymers as functional materials for electromechanical transducers. *Smart Materials and Structures* 23(3): 033001 (26 pp.).

Savolainen A and Kirjavainen K (1989) Electrothermomechanical film. Part I. Design and characteristics. *Journal of Macromolecular Science: Part A—Chemistry* 26(2–3): 583–591.

Wang Y, Wu L and Zhang X (2015) Energy harvesting from vibration using flexible floroethylenepropylene piezoelectret films with cross-tunnel structure. *IEEE Transactions on Dielectrics and Electrical Insulation* 22(3): 1349–1354.

Wegener M and Bauer S (2005) Microstorms in cellular polymers: a route to soft piezoelectric transducer materials with engineered macroscopic dipoles. *ChemPhysChem* 6(6): 1014–1025.

Wu N, Cheng X, Zhong Q, et al. (2015) Cellular polypropylene piezoelectret for human body energy harvesting and health monitoring. *Advanced Functional Materials* 25(30): 4788–4794.

Zhang X, Sessler GM and Wang Y (2014) Fluoroethylenepropylene ferroelectret films with cross-tunnel structure for piezoelectric transducers and micro energy harvesters. *Journal of Applied Physics* 116(7): 074109 (8 pp.).

Zhang X, Wu L and Sessler GM (2015) Energy harvesting from vibration with cross-linked polypropylene piezoelectrets. *AIP Advances* 5(7): 077185 (10 pp.).